

This is the submitted version of the following article:

Chikoidze E., Rogers D.J., Teherani F.H., Rubio C., Sauthier G., Von Bardeleben H.J., Tchelidze T., Ton-That C., Fellous A., Bove P., Sandana E.V., Dumont Y., Perez-Tomas A.. Puzzling robust 2D metallic conductivity in undoped  $\beta$ -Ga<sub>2</sub>O<sub>3</sub> thin films. *Materials Today Physics*, (2019). 8. : 10 - .  
10.1016/j.mtphys.2018.11.006,

which has been published in final form at  
<https://dx.doi.org/10.1016/j.mtphys.2018.11.006> ©  
<https://dx.doi.org/10.1016/j.mtphys.2018.11.006>. This  
manuscript version is made available under the CC-BY-NC-ND  
4.0 license  
<http://creativecommons.org/licenses/by-nc-nd/4.0/>

# **Puzzling robust 2D metallic conductivity in undoped $\beta$ -Ga<sub>2</sub>O<sub>3</sub> thin films**

E. Chikoidze<sup>1\*</sup>, D. J. Rogers<sup>2</sup>, F. H. Teherani<sup>2</sup>, C. Rubio<sup>3</sup>, G. Sauthier<sup>3</sup>, H. J. Von Bardeleben<sup>4</sup>

T. Tchelidze<sup>5</sup>, C. Ton-That<sup>6</sup>, A. Fellous<sup>1</sup>, P. Bove<sup>2</sup>, E. V. Sandana<sup>2</sup>, Y. Dumont<sup>1</sup>

and A. Perez-Tomas<sup>3</sup>

<sup>1</sup>Groupe d'Etude de la Matière Condensée (GEMaC), Université de Versailles Saint Quentin en Yvelines –  
CNRS, Université Paris-Saclay, 45 Av. des Etats-Unis, 78035 Versailles Cedex, France

<sup>2</sup>Nanovation, 8 route de Chevreuse, 78117 Châteaufort, France

<sup>3</sup>Catalan Institute of Nanoscience and Nanotechnology (ICN2), CSIC and The Barcelona Institute of Science  
and Technology, Barcelona, Spain

<sup>4</sup>Sorbonne Universités, UPMC Université Paris 6, Institut des Nanosciences de Paris, CNRS, 4, place  
Jussieu, 75005 Paris, France

<sup>5</sup>Faculty of Exact and Natural Science, Department of Physics, Ivane Javakhishvili Tbilisi State University, 3  
Av. I. Tchavtchavadze, 0179 Tbilisi, Georgia

<sup>6</sup>School of Mathematical and Physical Science, University of Technology Sydney, Broadway, PO Box 123,  
NSW 2007, Australia

## ABSTRACT

Here we report the analogous of an extremely stable *topological-like ultra-wide bandgap insulator*, (a solid that is a pure insulator in its bulk but has a metallic conductive surface), presenting a two-dimensional conductive channel at its surface that challenges our current thinking about semiconductor conductivity engineering. Nominally undoped epitaxial  $\beta$ -Ga<sub>2</sub>O<sub>3</sub> thin-films without any detectable defect (after a range of state-of-the-art techniques) showed the unexpectedly low resistivity of ( $3 \times 10^{-2} \Omega\text{cm}$ ) which was found to be also resistant to high dose proton irradiation (2MeV,  $5 \times 10^{15} \text{cm}^{-2}$  dose) and was largely invariant (metallic) over the phenomenal temperature range of 2K up to 850K. The unique resilience and stability of the electrical properties under thermal and highly ionising radiation stressing, combined with the extended transparency range (thanks to the ultra-wide bandgap) and the already known toughness under high electrical field could open up new perspectives for use as expanded spectral range transparent electrodes (e.g. for UV harvesting solar cells or UV LEDs/lasers) as well as robust Ohmic contacts for use in extreme environments/applications and for novel optoelectronic and power device concepts.

### 1. Introduction

Intriguing metallic surfaces onto otherwise insulating bulk crystals have recently attracted a lot of attention [1,2]. These conductive surfaces also exhibit a number of additional unique properties such as insulator–superconductor–metal transition[3], large magnetoresistance[4], coexisting ferromagnetism and superconductivity [5] and a spin splitting of a few meV [6]. In practice, as the oxide semiconductor bandgap becomes wider, an intrinsic metallic surface is more challenging; it is required more energy to shift the Fermi level from the mid-gap to above the conduction band as the forbidden gap increases.

Beta-gallium oxide (Ga<sub>2</sub>O<sub>3</sub>) is an ultra-wide band gap (UWBG) semiconductor with a highly distinctive property set compared to other classical correlated oxides such as SrTiO<sub>3</sub> [7-8], In<sub>2</sub>O<sub>3</sub> [9-10], CdO[11], or

ZnO[12]. The uniqueness of UWBG Ga<sub>2</sub>O<sub>3</sub> lies in the combination of an intrinsically wide large electrical breakdown field [13,14], ability to be efficiently donor doped [15-16], [possibility to obtain low resistivity also in amorphous and nano-crystalline states \[17-20\]](#), a high temperature *p*-type conductivity without doping[21] and 6-inch crystal low cost fabrication possibility [22]. These features have been key in promoting Ga<sub>2</sub>O<sub>3</sub> to the forefront in the quest for the next generation of UVC photodetectors, solar transparent conducting electrodes and high power/speed energy converters/switches.

Recently the authors reported unprecedentedly high conductivity, mobility and carrier concentration in nominally undoped thin films of grown on *r*-sapphire substrates by pulsed laser deposition (PLD). [23]

This work, presents evidence that the degenerate electrical conduction, in what was expected to be an insulating layer, may be due to two-dimensional like metallic conduction in  $\beta$ -Ga<sub>2</sub>O<sub>3</sub>. Moreover, the electrical conduction has now proven stable for over two years and shows a remarkable resistance to both thermal and radiation stressing.

[The ability to obtain ultra wide band gap undoped Gallium oxide highly transparent and the same time highly conducting makes this material as a very fascinating transparent conducting oxide \(TCO\), of key enabling materials in increasingly high demand in a variety of new technologies, ranging from thin film coatings, sensors, solar cells, transparent electronics and optoelectronics in telecommunications \[24\]](#) Additionally, Analogous of an extremely stable *topological-like ultra-wide bandgap insulator*, presenting a two-dimensional conductive channel at its surface challenges our current thinking about semiconductor conductivity engineering.

## 2. Intrinsic Ga<sub>2</sub>O<sub>3</sub>

Nominally undoped  $\beta$ -Ga<sub>2</sub>O<sub>3</sub> layers were grown on 2-inch *r*-plane sapphire substrates by PLD as described in Experimental section. The layers (~300 nm thick) were found to be epitaxial with a (201) preferential orientation. The wafers were found to be solar transparent in that they exhibited a large transmittance (> 85%) in the UVA, UVB and visible parts of the optical spectrum. The optical absorption edge gave an estimation of bandgap at about 240 nm (~5.2 eV). The surface and bulk chemical composition of the layers was systematically investigated by several high-resolution techniques (see methods and supplemental materials) including: X-ray photoemission spectroscopy (XPS), energy dispersive X-ray fluorescence spectroscopy (EDS), secondary ion mass spectroscopy (SIMS), and Rutherford backscattering spectrometry (RBS). The depth-resolved CL spectra of the Ga<sub>2</sub>O<sub>3</sub> film with identical excitation power, shown in Figure 5(Experimental Section), reveal a symmetrical peak at 3.3 eV. The UV emission band of the film is similar

to those observed for excitons immobilised by a local lattice deformation in a single  $\text{Ga}_2\text{O}_3$  single crystal [25]. The peak shape and energy position remain unchanged with increasing sampling depth by consequently accelerating voltage, indicating homogeneity in sample volume. In all cases, no significant density of impurities was detected. Room temperature electron paramagnetic resonance (EPR) [26] was also performed and did not detect any shallow donor related signal. Fig. 1 summarizes the main findings.

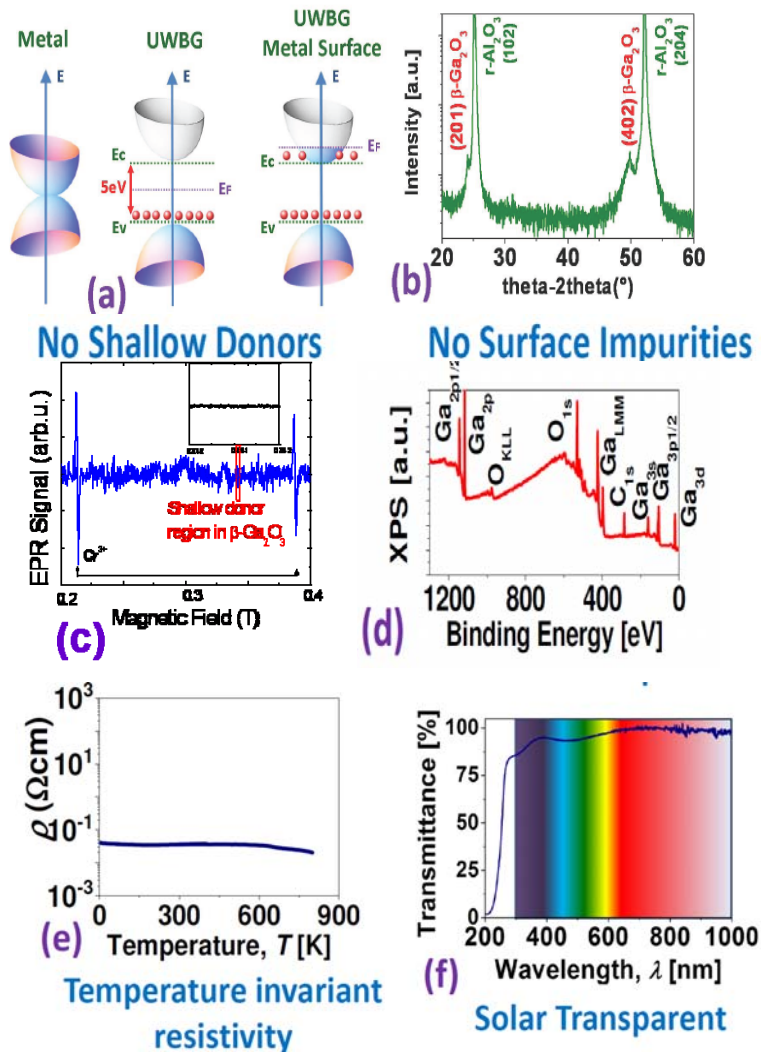


**Fig.1** (a). Sketch showing the band structure of the Ga<sub>2</sub>O<sub>3</sub> conductive surface. (b) The Ga<sub>2</sub>O<sub>3</sub> layers are epitaxial with (201) preferential orientation (XRD). There are no detectable (c) shallow donors (EPR) or (d) surface impurities (XPS). (e) The Ga<sub>2</sub>O<sub>3</sub> temperature invariant metallic conductivity. (f) The Ga<sub>2</sub>O<sub>3</sub> layers are solar transparent (80% transmittance in whole UVB, UVA and visible ranges).

### 3. Transport Properties – Low Temperature

The electrical transport properties of the films were studied in a Van der Pauw and “4 aligned point contacts” method configurations. The room temperature resistivity ( $\rho(300\text{K})$ ) was found to be exceptionally low for an intrinsic UWBG material ( $\rho(300\text{K}) = 3 \times 10^{-2} \Omega \cdot \text{cm}$  which is, to the best of our knowledge, the lowest reported value for undoped Ga<sub>2</sub>O<sub>3</sub> thin films and about equivalent to that for heavily *n*-type doped Ga<sub>2</sub>O<sub>3</sub> (Si or Sn doping in the range of  $10^{19}$ - $10^{20} \text{ cm}^{-3}$ )[23,25-31]. Fig. 2a. Hall effect measurements at room under 1 Tesla revealed an electron carrier concentration as high as  $n = 8.0 \times 10^{18} \text{ cm}^{-3}$  for a film thickness of 200 nm, and a mobility of  $\mu = 19 \text{ cm}^2/\text{Vs}$ . This value of  $8 \times 10^{18} \text{ cm}^{-3}$ , corresponds to the hypothesis of a thickness homogeneity of the electron carrier concentration. Such a relatively large free charge carrier concentration indicates that the Ga<sub>2</sub>O<sub>3</sub> undergoes a Mott metal-insulating (M-I) transition. In Ga<sub>2</sub>O<sub>3</sub>, a Mott M-I transition would occur at a dopant critical concentration of  $N_{Mott} = 4 \times 10^{18} \text{ cm}^{-3}$ , where  $N_{Mott}^{1/3} \times a_B \approx 0.27$  and  $a_B$  is the impurity Bohr radius ( $a_B(\text{Ga}_2\text{O}_3) = 1.8 \text{ nm}$ ). [32] We integrate over the film thickness, this corresponds to a surface carrier concentration of  $1.6 \times 10^{14} \text{ cm}^{-2}$ .

Fig. 2 (b) shows a representative resistance versus temperature curve measured with a colinear four point probe configuration. The resistance was found to be relatively temperature independent (over the full range from 2 K to 400 K) and there was no evidence of carrier freeze-out at lower  $T$ . Both characteristics are typical signatures of metallic conduction. The slight increase of resistivity observed above 200K is most probably attributable to a decrease in the drift mobility of free carriers. The “hockey stick” shape with a minimum at around  $T_{min} \sim 190 \text{ K}$  is then formed by a slight increase in resistivity at low temperatures, which is most probably due to a weak localization (WL) phenomenon which is related to low dimensional effects [33]. Due to the quantum interference, the electron wave functions diffuse and the backscattering is enhanced which, in turn, increases the resistivity as a function of  $\ln(T)$ . As shown in Fig. 2(c), the conductivity at low temperatures increases precisely as  $\ln(T)$  [34]. At higher temperatures, the wave coherence is progressively

lost and the WL effect gives place to metallic behaviour. Similar resistivity vs  $T$  dependence has been already reported for confined conductive channels in two-dimensional carbides and oxides such as TiC [35], ZnO [36], LaNiO<sub>3</sub>, [37] and SrVO<sub>3</sub> [38].

The WL effect is sensitive to an applied perpendicular magnetic field ( $B$ ), which shifts  $T_{min}$  towards lower temperatures[39], as shown in Fig 2b. The presence of a strong magnetic field perpendicular to the plane of the conduction channel also leads to a quenching of charge localization contribution and thus produces a negative magnetoresistance. [40] The magnetoresistance (MR) is defined as  $MR=[R(B)-R(B=0)]/R(B=0)$ , where  $R(B)$  is the resistance measured for  $B$  perpendicular to the applied current. The MR was found to be always negative at temperatures  $< 150$  K, and the maximum MR value was found to be 2.5 % at  $B = 9$  T (Fig. 2(d)). The field dependence up to a saturation of the negative MR at 2 K, is comparable with that observed for a 2D-like conduction in highly doped semiconductors layers .[40,41] Because of the relatively small value of mobility at low temperature, quantum oscillations would not be observable even at our highest available magnetic field (9T).

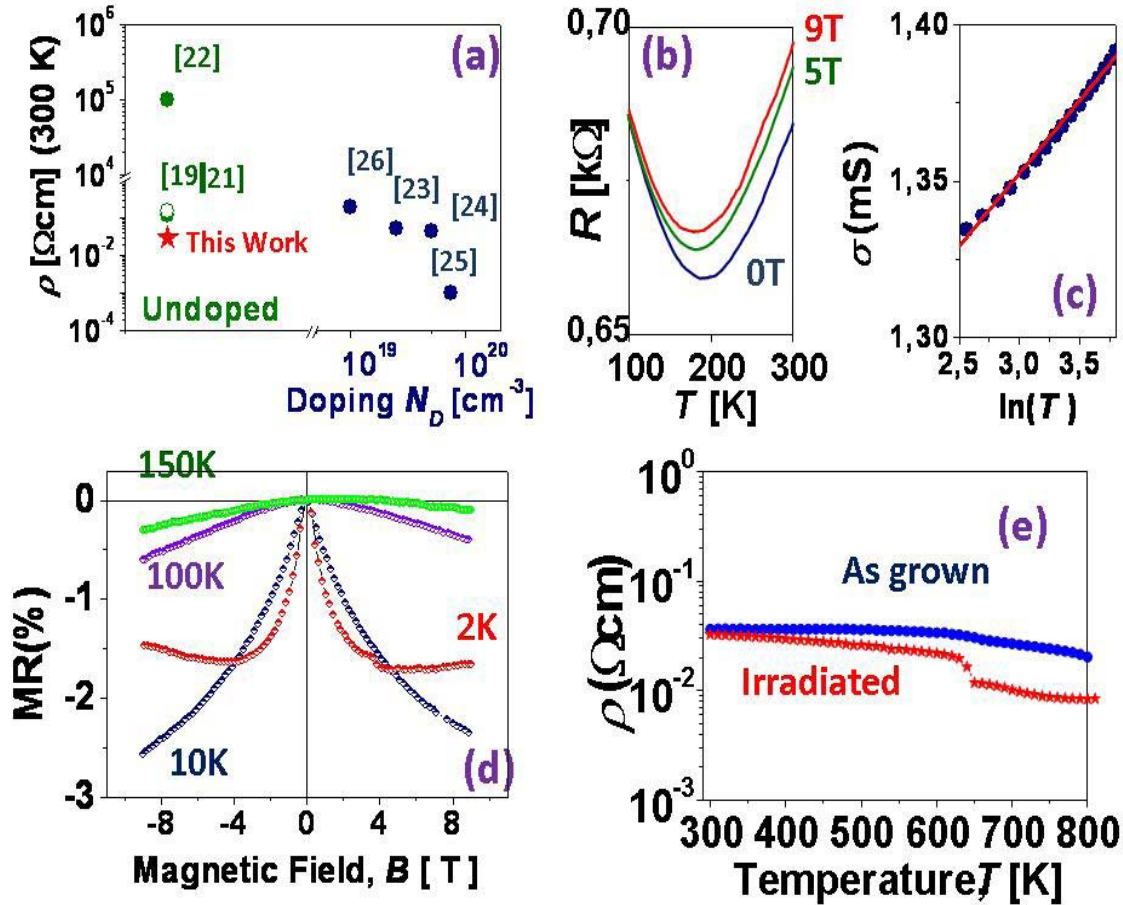


**Figure 2.** (a) Room temperature resistivity for our undoped Ga<sub>2</sub>O<sub>3</sub>/r-sapphire sample compared with other undoped and heavily Sn- or Si-doped Ga<sub>2</sub>O<sub>3</sub> results from literature<sup>[19,22-26]</sup>. (b) Zoom Electrical resistance versus temperature at 0T, 5T and 9T applied magnetic fields (c) Sheet conductance  $\sigma$  versus  $\ln(T)$  for up-rise part below the M-I transition temperature ( $T_{min}$ ) range. The solid line is the linear fit at *zero* magnetic field. (d) Magnetoresistance in perpendicular magnetic field at 2K, 10K, 100K and 150K. Measurement geometry: collinear 4 point probes. (e) Electrical resistivity versus temperature (300K-800K) for as grown and proton irradiated (2MeV,  $5 \times 10^{15} \text{cm}^{-2}$  dose) sample. Measurement configuration was Van der Pauw.



#### 4. High Temperature Electrical Transport Properties

The metallic Ga<sub>2</sub>O<sub>3</sub> conduction has been found to be stable and resistant to different stress conditions. Stored on the shelf during two years, it showed no degradation (or drift) after 10 subsequent  $R(T)$  characterization cycles. The conductive channel reversibly survived temperatures up to as high as 850 K (limit of the experimental set-up), showing only a small deviation of the resistivity at elevated temperature ( $\rho(850\text{K}) = 1.7 \times 10^{-2} \Omega\text{cm}$ ). Analogously, the sample was proton irradiated (2MeV,  $5 \times 10^{15} \text{cm}^{-2}$  dose) (see experimental section) Proton irradiation at these doses and energies would be expected to create oxygen (deep donor) and gallium (deep acceptor) bulk vacancies, thus changing overall conductivity by orders of magnitude [42]. However, as shown in Fig.2(e), the conductivity after irradiation only slightly decreases at high temperatures. As the free carrier concentration is most probably confined in a narrow region close to the surface of the layer, a metallic surface would be more resistant to radiation than bulk conductive samples where random electron-hole pairs would be formed. This high temperature stability is notable when compared with other correlated oxide systems such as confined 2D electrons metallic system (2DES) LaAlO<sub>3</sub> and SrTiO<sub>3</sub>. [43,44] Single-crystal In<sub>2</sub>O<sub>3</sub>, ZnO, and TiO<sub>2</sub> have been also reported to host a surface 2DES presenting however air-instabilities and practical electrical conduction only at low temperature (i.e., < 100 K). [45]

The resistivity versus temperature quasi invariance stability also ruled out other known non-surface origins of intrinsic Ga<sub>2</sub>O<sub>3</sub> conductivity; i.e. the presence of (1) amorphous phases or (2) gallium clusters. Regarding (1) a chemically driven M-I Ga<sub>2</sub>O<sub>3</sub> transition (of seven orders of magnitude) has been previously reported in highly non-stoichiometric, amorphous gallium oxide. [46] As we see from Fig.2 (b),  $R(T)$  curves showed no significant differences for subsequent heating and cooling cycles. This result excludes the possibility of solid state recrystallization reaction due to amorphous phases being present in the material. Regarding (2), gallium clusters (embedded into the Ga<sub>2</sub>O<sub>3</sub> matrix) would also result in resistivity temperature hysteresis due to melting and recrystallization of Ga clusters and a sharp drop of the resistivity at low  $T$  (<10

K) (attributed to superconducting state of gallium) [47]. Furthermore, Ga clusters would render the layers non transparent in the visible (coloration due to defects) [48]. Those features were not observed (Fig. 1d,1f) .

### 3. Electron accumulation in $\text{Ga}_2\text{O}_3$

The origin of the  $n$ -type intrinsic bulk conductivity for binary metal oxides (i.e., ZnO,  $\text{In}_2\text{O}_3$ ,  $\text{SnO}_2$  etc) is usually explained with a stoichiometric deviation: an anion (i.e. oxygen) deficiency or metallic cation interstitials. Therefore, intrinsic donors for intrinsic  $n$ -type conductivity in  $\text{Ga}_2\text{O}_3$  are the oxygen vacancy,  $\text{V}_\text{O}$ , and gallium interstitial,  $\text{Ga}_\text{i}$ . Hybrid functional calculations predict the  $\text{V}_\text{O}$  to be a deep donor with an ionization energy higher than 1eV in  $\text{Ga}_2\text{O}_3$ . [49] Hence, it is unlikely that bulk oxygen vacancies could be the source of the metallic conductivity observed in our experiment. Interstitial Ga atom  $\text{Ga}_\text{i}$  are relatively shallow donors with an ionization energy of 0.1-0.2 eV. However,  $\text{Ga}_\text{i}$  has very high formation energy [50] which also makes it an unlikely candidate. Because of the breaking of translational symmetry at the surface, an electronic state may exist with significantly different properties and characteristic energies than those in the bulk [51]. A particularly investigated case is  $\text{In}_2\text{O}_3$  surfaces (indirect bandgap of 2.5 eV and a direct bandgap of 3.6 eV).  $\text{In}_2\text{O}_3$  surface donors, (rather than bulk defects), are reported to be the source of its downwards band-bending and surface 2DEG. [52] In a similar fashion, surface electron accumulation was also observed on the surfaces of other binary wide bandgap oxides such as CdO ( $E_g \sim 2.18$  eV) and ZnO ( $E_g \sim 3.37$  eV) [53]. In the case of  $\text{Ga}_2\text{O}_3$ , a surface band bending phenomena due to surface defects was already pointed out by Lovejoy *et al.* [54]. Well known quantum Hall Effect in 2D semiconductors and oxides usually can be observed only in high-purity Si or GaAs at very low temperatures and strong magnetic fields and at room temperature only in graphene. [55]

When oxygen vacancies (or other surface donors) are present, surface positive charge causes a downward band bending; the extra electrons accumulate close to positive charges and create an accumulation layer in the near-surface region; the downward band bending causes a rigid shift of all peaks in the photoemission spectrum downwards. This shift has been reported to be of 0.2–0.3 eV in the case of reduced titania which is formally associated to the transformation of  $\text{Ti}^{4+}$  to  $\text{Ti}^{3+}$ . [56] On the contrary, surface acceptors cause upward band bending, accumulation of holes close to the surface and shift of the core levels towards lower binding energies (BE). XPS allowed the study of such core levels. The BE shifts in the O1s XPS spectra

result from the difference in the valences of the O<sup>2-</sup> ions. Lower BE indicates higher electron number at O-ions. The room temperature photoemission spectrum for the Ga2*p*, Ga3*p*, O1*s* and C1*s* core levels is shown in Fig. 3 (a). In this analysis, XPS spectra for our Ga<sub>2</sub>O<sub>3</sub> layer surface (labelled *n*-type) are compared with; (1) a control sample of commercial (Novel Crystal Technology, Inc.) nominally *n*-type Si-doped β-Ga<sub>2</sub>O<sub>3</sub> ( $N_d - N_a = 1.3 \times 10^{18} \text{ cm}^{-3}$ ) epitaxy (500 nm) grown on a single crystal β-Ga<sub>2</sub>O<sub>3</sub> (labelled Ref) and (2) a *p*-type Ga<sub>2</sub>O<sub>3</sub> surface (containing gallium vacancies) from Nanovation. [21] The BE value of the core level for the Ga2*p* states at 1119.3 eV (as determined by Michling et al. [57] for cleaved β-Ga<sub>2</sub>O<sub>3</sub> single crystals) were used to calibrate the BE positions of the XPS spectra. As shown in Fig. 3(b), the Ga<sub>2</sub>O<sub>3</sub> BE shift ( $\Delta BE = BE - BE_{ref}$ ) with respect to the Si-doped Ga<sub>2</sub>O<sub>3</sub> Ref correlates well with an *n*-type electron surface accumulation and a *p*-type electron depletion. The *n*-type Ga<sub>2</sub>O<sub>3</sub> sample exhibits a shift towards higher BE energy values while the *p*-type sample exhibits a shift towards lower BE values for both anions and cations.

Therefore, as the peaks of all the elements shift the BE in the same direction, it is deduced that the BE shift is dominated by raising/lowering of the chemical potential (i.e. the potential shift due to surface oxygen vacancies or metal interstitials). It is worth mentioning that the XPS for the Ga2*p* core level spectrum show no appreciable shoulder-like feature for either Ga2*p*<sub>1/2</sub> or Ga2*p*. When the Ga atom occupies an interstitial site, it is surrounded by more oxygen atoms. Therefore, cation shoulder-like features could be treated as direct evidence for the presence of interstitials. The evidence of the BE shift coupled with the absence of shoulder-like features for Ga peaks suggest that the origin of the donors in the *n*-type layers are due to oxygen vacancies.

From valence band photoemission spectra, it is possible to determine the electronic surface properties of the thin-films. The three maxima of the O<sup>2*p*</sup> valence band correspond to the three different oxygen sites in β-Ga<sub>2</sub>O<sub>3</sub> (O(1), O(2) and O(3)). The valence band width for the reference sample is ~8 eV, which is in agreement with previous reports. [58] The extrapolation of the first slope (at ~5 × 10<sup>2</sup> counts/s) gives Fermi levels of 4.9 eV and 4.4 eV, respectively, for the Ga<sub>2</sub>O<sub>3</sub> metallic surface (*n*-type) and the Si-doped control (Ref) samples. Therefore, the Fermi level for the metallic surface was experimentally confirmed to be above the conduction band edge (i.e. degenerately doped electron accumulation) if one assumes the usual bandgap value of 4.8 eV given in the literature. [59] Ultraviolet photoelectron spectroscopy (UPS) also corroborates the degenerately doped Fermi level position at ~4.9 eV as shown in Fig. 3(e).

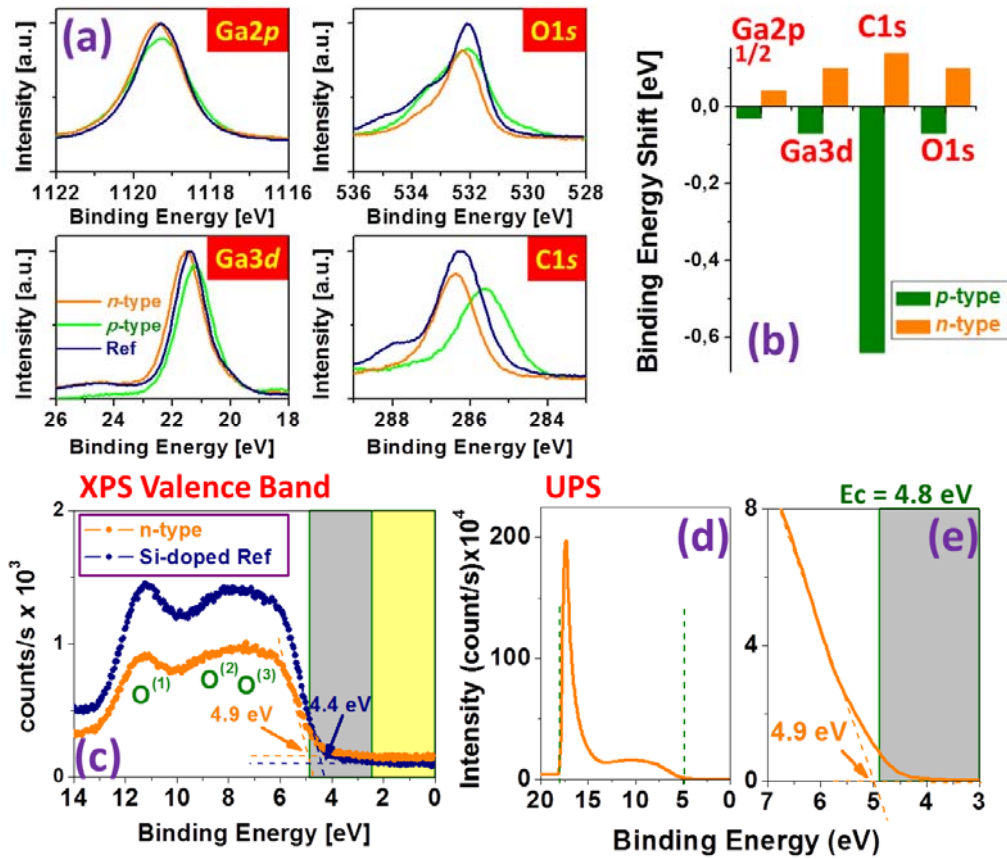


**Figure 3.** (a) XPS photoemission spectra for the Ga2p, Ga3p, O1s and C1s core levels for n-type studied sample, *p*-type [21] and Si doped reference. (b) *n*-type and *p*-type binding energy shift ( $\Delta BE = BE - BE_{ref}$ ) with respect to the control Si-doped Ga<sub>2</sub>O<sub>3</sub>. (c) Valence band photoemission spectra for *n*-type and Ref showing that our sample surface is degenerately conductive. (d) UPS spectra of the surface of the undoped conductive surface. (e) Zoom at conduction band edge.

### Theoretical estimation of carrier accumulation

The 2DEG free electron concentration density profile can be estimated by the Thomas-Fermi approximation for a 2D system (see supplementary information).[60] It is possible to find a relationship between the surface Fermi level (measured from the band edge) and the bulk three-dimensional electron density using:

$$E_F = \left(3\pi^2\right)^{2/3} \frac{\hbar^2}{2m_e^*} n^{2/3} \quad (2)$$

where  $E_F$  is the average difference between the Fermi energy and the band gap potential  $V(z)$ , which changes along the  $z$ -axis (the  $z$ -axis being perpendicular to the sample surface). Therefore,

$$E_F - V(z) = \left(3\pi^2\right)^{2/3} \frac{\hbar^2}{2m_e^*} n(z)^{2/3} \quad (3)$$

Setting the energy to zero at  $E_F$ , Poisson's equation for near surface potential energy is (neglecting fixed charges):

$$\frac{d^2V}{dz^2} = \frac{1}{3\pi^2} \left(\frac{e^2}{\epsilon_r \epsilon_0}\right) \left(\frac{2m_e^*}{\hbar^2}\right)^{3/2} (-V)^{3/2} \quad (4)$$

for which solutions are,

$$V(z) = -\frac{b}{(z+z_0)^4}, \quad b = \left(\frac{60\pi^2 \epsilon_r \epsilon_0}{e^2}\right)^2 \left(\frac{\hbar^2}{2m_e^*}\right)^3 \quad (5)$$

$$n(z) = \frac{a}{(z+z_0)^6}, \quad a = \left(\frac{2m_e^* b}{\hbar^2}\right)^{3/2} \quad (6)$$

$$n(z) = \frac{a}{(z+z_0)^6}, \quad a = \left(\frac{2m_e^* b}{\hbar^2}\right)^{3/2} \quad (6)$$

In Eq. (5-6)  $z_0$  is defined by the boundary condition value of  $V(0)$ . Band bending at the surface  $BB$  was used for determining it. For  $BB$  :

$$BB = E_{v-F}^S - E_{v-F}^B = E_{v-F}^S - (E_g - E_{c-F}^B) \quad (7)$$

Where  $E_{v-F}^S$  and  $E_{v-F}^B$  are the top of valence band to Fermi energy distance at the surface and in the bulk respectively. The latter can be expressed as the sum of bulk band gap,  $E_g$ , and the distance between the Fermi energy and the bottom of conduction band in the bulk material. In Ref. 55 temperature narrowing of the bandgap in  $\text{Ga}_2\text{O}_3$  is studied and a 4.65 eV room temperature bandgap is reported; our electron concentration corresponds to  $E_{c-F}^B = 0.05$  eV.

As the zero of energy is at  $E_{c-F}^B$

$$V(0) = -(BB + E_{c-F}^B) = -(E_{v-F}^S - E_g) \quad (8)$$

In our case

$$V(0) = -0.25\text{eV}, \quad BB = 0.2\text{eV}.$$

Taking into account the experimental XPS and UPS Fermi level of 4.9 eV, an estimation of the characteristic depth profile for the bandgap potential ( $V(z)$ ) and 2DEG density ( $n(z)$ ) may be determined as shown in Fig. 4 (a,b). The calculated concentration of surface electrons  $n(0) = 10^{21} \text{ cm}^{-3}$ , with an average concentration  $n_{av} \sim 10^{19} \text{ cm}^{-3}$  matches well with the free electron concentration estimated in the Hall effect. The calculated electron concentration drops to  $\sim 10^{19} \text{ cm}^{-3}$  at a depth of  $z = 5$  nm, which represents roughly two  $\text{Ga}_2\text{O}_3$  unit cells (Fig. 4(c)). Under this approximation, the sheet charge concentration of the 2DEG is  $ns \sim 2 \times 10^{14} \text{ cm}^{-2}$ . Such a high value of sheet charge density induces a large diffusion of carriers and, consequently, a low value of mobility. This is the reason why no quantum oscillations are seen as a function of temperature and magnetic field in the available ranges. This may be further investigated. Nevertheless, the robust metallic

conduction, appears to be connected with surface band bending, as already observed in other oxide semiconductor surfaces.

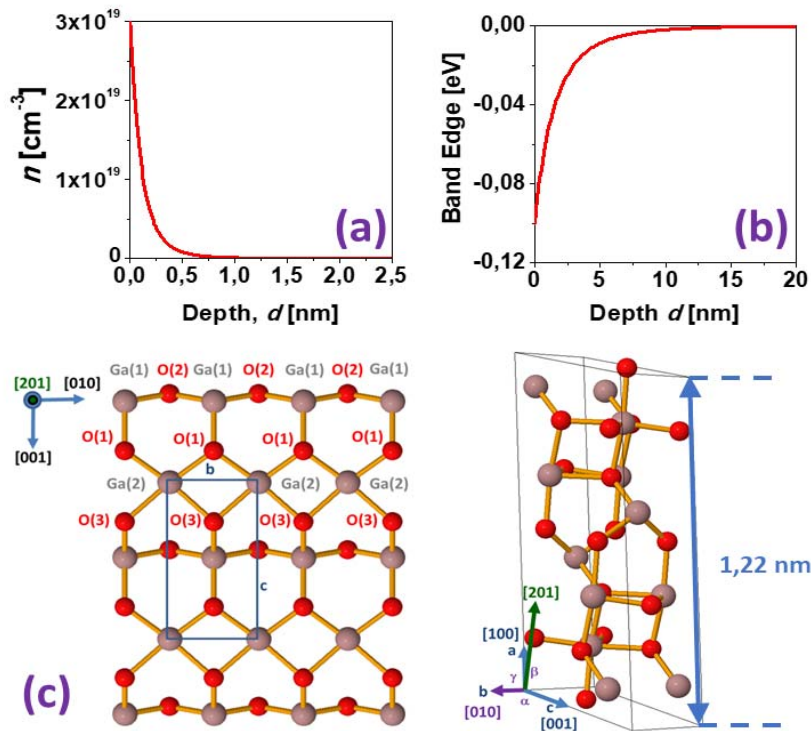


**Figure 4.** (a), (b) Simulated two-dimensional channel profile using the Thomas-Fermi approximation. (c) Sketch of the (201) plane and the Ga<sub>2</sub>O<sub>3</sub> unit cell.

## CONCLUSIONS

In this work, temperature dependent electrical transport measurements revealed that than nominally undoped  $\beta$ -Ga<sub>2</sub>O<sub>3</sub> thin films exhibited degenerate metallic conduction with a room temperature Hall  $n$  of  $8 \times 10^{18} \text{ cm}^{-3}$  and Hall  $\mu$  of  $19 \text{ cm}^2/\text{Vs}$ . A number of high resolution techniques did not reveal any bulk or shallow donor signatures that could explain the conductivity in terms of conventional impurity or defect doping. The conductivity vs temperature was found to be unprecedentedly stable over the range from a few K to 850 K (limit of the measurement set-up), both, in air and nitrogen ambient and insensitive to high dose of proton irradiation ( $2\text{MeV}$ ,  $5 \times 10^{15} \text{ cm}^{-2}$  dose). These suggested that the electrical conduction was mainly confined to the layer close to the surface. Photoelectron spectroscopy and *hockey stick-like* behavior in low temperature magnetoresistance studies were also coherent with a 2D like conduction. The origin of a such exceptionally robust conduction merits to be investigated more deeply, since this exceptional result challenges our current understanding and methods to achieve, solar transparent conducting electrodes, Ohmic contacts and potential transistor conductive channels in a wide bandgap insulator which is now considered to be a key enabler of a sustainable and greener future.

## Experimental section

### Fabrication Details

**Ga<sub>2</sub>O<sub>3</sub> Epilayer.** Nominally undoped  $\beta$ -Ga<sub>2</sub>O<sub>3</sub> layers were grown on 2-inch diameter *r*-plane sapphire substrates from a commercial sintered 4N Ga<sub>2</sub>O<sub>3</sub> target using a Coherent LPX KrF ( $\lambda = 248\text{nm}$ ) laser by pulsed laser deposition (PLD). Uniform 2-inch diameter wafer coverage was obtained using optical rastering of the incident laser beam. Substrate temperature during growth was measured with a thermocouple to be  $\sim 550^\circ\text{C}$  and the ambient during growth was  $10^{-4}$  torr of molecular oxygen. Ga<sub>2</sub>O<sub>3</sub> layers were epitaxial, showing (201) preferential orientation [23]. [The relative low temperature \(i.e. T=500-550°C\) is enough for Ga<sub>2</sub>O<sub>3</sub> complete crystallization as reported previously by several groups \[61-64\]. However the crystallization temperature may vary from one set-up to another as other authors has reported that larger temperatures are required to avoid amorphous phase. \[65-66\]](#)



## Characterization Methods

**X-ray diffraction (XRD).** The crystallographic structure of the films was analysed with a Siemens D-5000 diffractometer using Cu-K $\alpha$  radiation ( $\lambda = 1.54 \text{ \AA}$ ).

**Interferometry.** The thickness of the gallium oxide layers was around 300 nm, estimated using optical reflection interferometry with an Ocean Optics Nanocalc system. The layer thickness was further corroborated with cross-sectional **scanning electronic microscopy (SEM)** FEI Quanta 650F Environmental SEM equipped with **energy dispersive X-ray spectroscopy (EDX)** for point analysis and chemical maps.

**Electron Spin Resonance (ESR)** measurements have been performed with a Bruker X-band spectrometer under standard conditions: 100 kHz field modulation and low ( $\mu\text{W}$ ) microwave power to avoid nuclear polarization effects. Only 2 transitions corresponding to a Cr contamination of the Al $_2$ O $_3$  substrate were observed.

**Secondary-ion mass spectrometry (SIMS)** was carried out with the aid of using a Cameca IMS 4f tool equipment.

**X-ray photoelectron spectroscopy (XPS) and ultraviolet photoelectron spectroscopy (UPS)** measurements were performed with a Phoibos 150 analyzer (SPECS GmbH, Berlin, Germany)) in ultra-high vacuum conditions (base pressure  $3 \times 10^{-10}$  mbar). XPS measurements were performed with a monochromatic Al K $\alpha$  X-ray source (1486.74 eV). UPS measurements were realized with a monochromatic HeI UV source (21.2 eV). Optical transmission spectra were measured in 200-2000 nm spectral range with a Perkin Elmer 9 spectrophotometer.

**Transport measurements.** Electrical contacts were made by soldering indium. As verified by I-V measurements, all contacts showed Ohmic I/V characteristics. DC-resistivity and magnetoresistance were studied using a commercial “DC-resistivity” configuration in a 9T-PPMS (Quantum Design Inc.) environment, while for high temperature ( $T > 300\text{K}$ ) measurements a home-designed high impedance measurement set-up was used. Magnetoresistance measurements were made with a magnetic field,  $B = \mu_0 H$ , applied perpendicular to the film plane. Hall effect measurements were performed in the Van der Pauw configuration for perpendicular magnetic fields of up to 1.6 T.

**Proton Irradiation.** Proton irradiation was performed with a Van de Graaff 2.5MV accelerator. A proton energy of 2MV was chosen in order to generate a homogeneous defect profile over the entire film and put the end of range in the sapphire substrate. The total fluence was  $1 \times 10^{16} \text{ cm}^{-2}$ . The current was  $1 \text{ microA/cm}^2$ , a value for which the film is expected to stay close to room temperature.

**ACKNOWLEDGEMENTS:** The authors acknowledge financial support from the Ile de France region ("NOVATECS" C'Nano IdF Project No? IF-08-1453.R) and from the French National Research Agency (ANR) as part of the "Investissements d'Avenir" program (Labex charmmmat, ANR-11-LABX-0039-grant). APT acknowledges Agencia Estatal de Investigación (AEI) and Fondo Europeo de Desarrollo Regional under contract ENE2015-74275-JIN. The ICN2 is funded by the CERCA programme / Generalitat de Catalunya and by the Severo Ochoa programme of the Spanish Ministry of Economy, Industry and Competitiveness (MINECO, grant no. SEV-2013-0295). TT acknowledges Shota Rustaveli National Science Foundation, grant #04/04.

We express our thanks to Dr. F. Jomard (GEMaC laboratory, CNRS-UVSQ) for SIMS measurements.

#### **AUTHOR INFORMATION**

\*E-mail: [ekaterine.chikoidze@uvsq.fr](mailto:ekaterine.chikoidze@uvsq.fr). Tel: +33-29-0139255025

#### **REFERENCES**

- [1] E.S. Reich , Hopes surface for exotic insulator, Nature 13 (2012) 492
- [2] T. C. Rödel , F. Fortuna , S. Sengupta , Emmanouil Frantzeskakis , P. Le Fèvre , F. Bertran , B. Mercey , Sylvia Matzen , G. Agnus, T. Maroutian , P. Lecoœur , A. F. Santander-Syro, Universal Fabrication of 2D Electron Systems in Functional Oxides, Adv. Mater. 28, (2016) 1976
- [3] J.He, D.Di Sante, R. Li, X-Q. Chen, J. M. Rondinelli , C. Franchini, Tunable metal-insulator transition, Rashba effect and Weyl Fermions in a relativistic charge-ordered ferroelectric oxide, Nature Communications 9, (2018)492
- [4] R.von Helmolt, J. Wecker, B. Holzapfel, L. Schultz, and K. Samwer, Giant negative magnetoresistance in perovskitelike  $\text{La}_{2/3}\text{Ba}_{1/3}\text{MnO}_x$  ferromagnetic films, Phys. Rev. Lett. 71 (1993)2331

- [5] Bednorz, J. G. & Muller, K. A., Perovskite-type oxides—The new approach to high-Tc superconductivity *Rev. Mod. Phys.* 60 (1988)585
- [6] A. F. Santander-Syro, F. Fortuna, C. Bareille, T. C. Rödel, G. Landolt, N. C. Plumb, J. H. Dil, M. Radović, Giant spin splitting of the two-dimensional electron gas at the surface of SrTiO<sub>3</sub>, *Nature Materials* 13 (2014) 1085
- [7] Yuhang Wang, Kehan Zhao, Xiaolan Shi, Geng Li, Guanlin Xie, Xubo Lai, Jun Ni, and Liuwan Zhang, Mechanical writing of n-type conductive layers on the SrTiO<sub>3</sub> surface in nanoscale, *Sci Rep.* 5 (2015)10841
- [8] D. S. Deak, Strontium titanate surfaces, *Mat.Science and Techn.* Volume 23 (2007) 127
- [9] D.R. Hagleitner, M. Menhart, P. Jacobson, S.Blomberg, K. Schulte, E. Lundgren, M. Kubicek, J.Fleig, F.Kubel, C. Puls, A. Limbeck, H. Hutter, L. A. Boatner, M.Schmid, U. Diebold, Bulk and surface characterization of In<sub>2</sub>O<sub>3</sub>(001) single crystals, *Phys Rev B* 85 (2012) 115441
- [10] P. Agoston, P. Erhart, A. Klein, and K. Albe, Geometry, electronic structure and thermodynamic stability of intrinsic point defects in indium oxide *J. Phys. Condens.Matt.* 21 (2009) 455801
- [11] J.Santos-Cruz, G.Torres-Delgado, R.Castanedo-Perez, S.Jiménez-Sandoval, O.Jiménez-Sandoval, C.I.Zúñiga-Romero, J.Márquez Marín, O.Zelaya-Angel, Optical and electrical characterization of fluorine doped cadmium oxide thin films prepared by the sol–gel method, *Thin Solid Films* 515 (2007) 5381
- [12] G.Luka, T.Krajewski, L.Wachnicki, B.Witkowski, E.Lusakowska, W.Paszkwicz, E. Guziewicz, M. Godlewski, Transparent and conductive undoped zinc oxide thin films grown by atomic layer deposition *Phys.Stat.sol.(a)* 207 (2010) 1568
- [13] M. Higashiwaki, K. Sasaki, A. Kuramata, T. Masui, and S. Yamakoshi, Gallium oxide (Ga<sub>2</sub>O<sub>3</sub>) metal-semiconductor field-effect transistors on single-crystal  $\beta$ -Ga<sub>2</sub>O<sub>3</sub> (010) substrates *Appl. Phys. Lett.* 100 (2012) 013504
- [14] A.J.Green, K. D. Chabak, M. Baldini, N.Moser, R. Gilbert, R. C. Fitch, G. Wagner, Z. Galazka, J. McCandless, A.Crespo, K. Leedy, G. H. Jessen,  $\beta$ -Ga<sub>2</sub>O<sub>3</sub>MOSFETs for RadioFrequency Operation, *IEEE ELECTRON DEVICE LETTERS*, 38 (2017)790
- [15] S. I. Stepanov, V. I. Nikolaev, V. E. Bourgov, A. E. Romanov, Gallium oxide: properties and application, *Rev. Adv. Mater. Sci.* 44 (2016) 63
- [16] S. J. Pearton, J. Yang, P. H. Cary, F. Ren, J. Kim, M. J. Tadjer, M.A. Mastro, A review of Ga<sub>2</sub>O<sub>3</sub> materials, processing, and devices, *Appl.Phys. Rev.* 5 (2018) 011301
- [17] L.I.Juarez-Amador, M.Galvan-Arellano, J.a.Andraca-Adame, G.Romero-paredas, A.kennedy-Magos, R.Pena-sierra, *J.materials Science:mat.in Electronics*, 18 (2018) 1
- [18] C.V.ramana, E.J.Rubio, C.D.Barraza, a.Miranda Gallardo, S.McPeack, S.Kortu, J.T.Grant, *J.Appl.Phys.* 115 (2014) 043508
- [19] M.D.Heinemann, J.Berry, G.Teeter, T.Unold, D.Ginley, Oxygen deficiency and Sn doping of amorphous Ga<sub>2</sub>O<sub>3</sub>, *Appl.Phys.Lett.* 108 (2016) 022107

- [20] J.Kim, T.Sekiya, N.Miyokawa, N.Watanabe, K.Kimoto, K.Ide, Y.Toda, Sh.Ueda, N.Ohashi, H.Hiramatsu, H.Hosono, Conversion of an ultra-wide bandgap amorphous oxide insulator to a semiconductor, *NPG Asia materials*, 9 (2017) e359
- [21] E.Chikoidze, A. Fellous, A. Perez-Tomas., Sauthier G., T.Tchelidze , C. Ton-That., T.Thanh Huynh, Phillips M., S.Russell, Jennings M., Berini B., Jomard F., Y. Dumont, P-type  $\beta$ -gallium oxide: A new perspective for power and optoelectronic devices, *Materials Today Physics*, 3 (2017)118
- [22] M.Orita H. Hiramatsu , H. Hosono , Preparation of highly conductive, deep ultraviolet transparent  $\beta$ -Ga<sub>2</sub>O<sub>3</sub> thin film at low deposition temperatures, *Thin Sol.Films*, 411 (2002)134
- [23] F.H. Teherani, D. J. Rogers, V. E. Sandana, P. Bove, C. Ton-That, L. L. C. Lem, E. Chikoidze, M. Neumann-Spallart, Y. Dumont, T. Huynh, M. R. Phillips, P. Chapon, R. McClintock, M. Razeghi, Investigations on the substrate dependence of the properties in nominally-undoped  $\beta$ -Ga<sub>2</sub>O<sub>3</sub> thin films grown by PLD, *Proc. of SPIE 10105* (2017), 10105R
- [24] R.M. Pasquarelli, David S. Ginley, Ryan O'Hayre, Solution processing of transparent conductors: from flask to film, *Chem. Soc. Rev.*, **40** (2011) 5406
- [25] K. Shimamura, E. G. Villora, T. Ujiie, and K. Aoki, Excitation and photoluminescence of pure and Si-doped  $\beta$ -Ga<sub>2</sub>O<sub>3</sub> single crystals ,*Appl. Phys. Lett.* 92 (2008)201914
- [26] M. Yamaga, E. G. Villora, K. Shimamura, N. Ichinose, M. Honda , Donor structure and electric transport mechanism in  $\beta$ -Ga<sub>2</sub>O<sub>3</sub> *Phys. Rev. B* 68 (2003) 155207
- [27] Sin-Liang Ou, Dong-Sing Wuu, Yu-Chuan Fu, Shu-Ping Liu, Zhe-Chuan Feng, Growth and etching characteristics of gallium oxide thin films by pulsed laser deposition *Mat.chem.Phys*, 133, (2012)700
- [28] K. Matsuzaki , H. Hiramatsu , K. Nomura , H. Yanagi ,T. Kamiya, M. Hirano, H. Hosono , Preparation of highly conductive, deep ultraviolet transparent  $\beta$ -Ga<sub>2</sub>O<sub>3</sub> thin film at low deposition temperatures, *Thin Solid Films* 496 (2006) 37
- [29] Wei Mi, Xuejian Du, Caina Luan, Hongdi Xiao, Jin Ma, Electrical and optical characterizations of  $\beta$ -Ga<sub>2</sub>O<sub>3</sub>:Sn films deposited on MgO (110) substrate by MOCVD, *RSC Adv.*, (2014) 4 30579
- [30] N. Suzuki, S. Ohira1, M. Tanaka, T. Sugawara, K. Nakajima, and T. Shishido, Fabrication and characterization of transparent conductive Sn-doped  $\beta$ -Ga<sub>2</sub>O<sub>3</sub> single crystal *phys. stat. sol. (c)* 4 (2007) 2310
- [31] Kevin D. Leedy, Kelson D. Chabak, V. Vasilyev, D. C. Look, J. J. Boeckl, J. L. Brown, S. E. Tetlak, A. J. Green, N. A. Moser, A. Crespo, D. B. Thomson, R. C. Fitch, J. P. McCandless, G.H. Jessen, Highly conductive homoepitaxial Si-doped Ga<sub>2</sub>O<sub>3</sub> films on (010)  $\beta$ -Ga<sub>2</sub>O<sub>3</sub> by pulsed laser deposition, *Appl.Phys.lett.* 111 (2017)012103
- [32] E. Chikoidze, H .J. von Bardeleben, K. Akaiwa, E. Shigematsu, K. Kaneko, S. Fujita, Y. Dumont, Electrical, optical, and magnetic properties of Sn doped  $\alpha$ -Ga<sub>2</sub>O<sub>3</sub> thin films, *J. Appl. Phys.* 120 (2016) 025109
- [33] G. Herranz, F.Sanchez, B.Martinez, J. Fontcuberta, M.V.Garcia-Cuenca, C. Ferrater, M. Varela, P.Levy, *Eur. Phys. J.* **2004**, B40, 439
- [34] Z. Q. Liu, D. P. Leusink, X. Wang, W. M. Lü, K. Gopinadhan, A. Annadi, Y. L. Zhao, X. H. Huang, S. W. Zeng, Z. Huang, A. Srivastava, S. Dhar, T. Venkatesan, and Ariando, *Phys. Rev. Lett.* 107 (2011) 146802
- [35] J. Halim, M.R. Lukatskaya,, K. M. Cook, J.Lu, C.R. Smith, L-A Näslund, S. J. May, L.Hultman, Y. Gogotsi, P.Eklund,,M.W. Barsoum, *Chem. Mater.* 26 (2014) 2374

- [36] M. Nistor, F. Gherendi, N. B. Mandache, C. Hebert, J. Perriere, W. Seiler, Metal-semiconductor transition in epitaxial ZnO thin films, *J. Appl. Phys.* 106 (2009) 103710
- [37] W. Noun, B. Berini, Y. Dumont, P.R. Dahoo, N. Keller, Correlation between electrical and ellipsometric properties on high-quality epitaxial thin films of the conductive oxide LaNiO<sub>3</sub> on STO (001) *J. Appl. Phys.* 102 (2007) 063709
- [38] M. Gu, S. A. Wolf, J. Lu, Two-Dimensional Mott Insulators in SrVO<sub>3</sub> Ultrathin Films, *Adv. Mater. Interfaces* (2014) 1300126
- [39] E. Rozenberg, M. Auslender, I. Felner, G. Gorodetsky, Low-temperature resistivity minimum in ceramic manganites, *J. Appl. Phys.* 88 (2000) 2578
- [40] S. Ashburn, R.A. Webb, E.E. Mendez, L.L. Chang, L. Esaki, *Phys Rev* 29 (1984) 3752
- [41] S. Kawaji, Weak localization and negative magnetoresistance in semiconductor two-dimensional systems, *Surf. Sci.* 170 (1986) 682
- [42] S. Ahn, Y-H Lin, F. Ren, S. Oh, Y. Jung, G. Yang, J. Kim, M.A. Mastro, J. K. Hite, Ch.R. Eddy, Jr. Stephen, J. Pearton, *J. Vac. Sci. Technol. B* 34 (2016) 041213
- [43] S.Y. Moon, Ch.W. Moon, H. J. Chang, T. Kim, Ch-Y., Kang, H-J. Choi, J-S. Kim, S-Hyub Baek, H.W. Jang, Thermal stability of 2DEG at amorphous LaAlO<sub>3</sub>/crystalline SrTiO<sub>3</sub> heterointerfaces *Nano Convergence* 12 (2016) 243
- [44] M. Huijben, A. Brinkman, G. Koster, G. Rijnders, H. Hilgenkamp, D.H.A. Blank, Structure-Property relation of SrTiO<sub>3</sub>/LaAlO<sub>3</sub> interfaces, *Adv. Mater* 21 (2009) 1665
- [45] Sang Yeon Lee, J. Kim, A. Park, J. Park, H. Seo, Creation and Control of Two-Dimensional Electron Gas Using Al-Based Amorphous Oxides/SrTiO<sub>3</sub> Heterostructures Grown by Atomic Layer Deposition, *ACS Nano* 11 (2017) 6040
- [46] L. Nagarajan, R. A. De Souza, D. Samuelis, I. Valov, A. Börger, J. Janek, K. Becker, P.C. Schmidt M. Martin, A chemically driven insulator-metal transition in non-stoichiometric and amorphous gallium oxide *Nature Mat.* 7 (2008) 391
- [47] C. Hebert, A. Petitmangin, J. Perrière, E. Millon, A. Petit, L. Binet, P. Barboux, *Materials Chemistry and Physics* 133 (2012) 135
- [48] A. Petitmangin, B. Gallas, C. Hebert, J. Perriere, L. Binet, P. Barboux, X. Portier, Characterization of oxygen deficient gallium oxide films grown by PLD, *Appl. Surf. Science* 278 (2013) 153
- [49] J. B. Varley, J. R. Weber, A. Janotti, C. G. Van de Walle, *J. Appl. Phys. Lett* 97, 142106 (2010)
- [50] V Wang, W Xiao, L-J Kang, R-J Liu, H Mizuseki and Y Kawazoe, Sources of n-type conductivity in GaInO<sub>3</sub>, *J. Phys. D: Appl. Phys.* 48 (2015) 015101
- [51] P. D. C. King, T. D. Veal, C. F. McConville, J. Zuñiga-Pe´rez,<sup>2</sup> V. Mun˜oz-Sanjose´,<sup>3</sup> M. Hopkinson,<sup>4</sup> E. D. L. Rienks, M. Fuglsang Jensen, Ph. Hofmann, Surface Band-Gap Narrowing in Quantized Electron Accumulation Layers, *PRL* 104 (2010) 256803
- [52] Phil D, C. King, T. D Veal, Conductivity in transparent oxide semiconductors, *J. Phys.: Condens. Matter* 23 (2011) 334214

- [53] S. Lany, A. Zakutayev, T. O. Mason, J. F. Wager, K. R. Poeppelmeier, J. D. Perkins, J. J. Berry, D. S. Ginley, A. Zunger, Surface Origin of High Conductivities in Undoped  $\text{In}_2\text{O}_3$  Thin Films *Phys. Rev. Lett.* 108, (2012) 016802
- [54] T. C. Lovejoy, R. Chen, X. Zheng, E. G. Villora, K. Shimamura, H. Yoshikawa, Y. Yamashita, S. Ueda, K. Kobayashi, S. T. Dunham, F. S. Ohuchi, and M. A. Olmstead, Band bending and surface defects in  $\beta\text{-Ga}_2\text{O}_3$  *Appl. Phys. Lett.* 100 (2012) 181602
- [55] J. Wang, F. Ma, W. Liang, M. Sun, *Materials Today Physics* 2 (2017) 6
- [56] *Defects at Oxide Surfaces*, Ed. J. Jupille and G. Thornton, Springer, Heidelberg (2015)
- [57] M. Michling and D. Schmeißer, Resonant Photoemission at the O1s threshold to characterize  $\beta\text{-Ga}_2\text{O}_3$  single crystals. *IOP Conference Series: Materials Science and Engineering* 34 (2012) 012002.
- [58] C. Janowitz, V. Scherer, M. Mohamed, A. Krapf, H. Dwelk, R. Manzke, Z. Galazka, R. Uecker, K. Irmscher, R. Fornari, *New J. Phys.* 13 (2011) 085014
- [59] *Low-Dimensional Semiconductor Structures: Fundamentals and Device Applications*, by Keith Barnham, Dimitri Vvedensky, Cambridge; New York : Cambridge University Press, (1943) 393 pages
- [60] S. Rafique, L. Han, Sh. Mou, and H. Zhao, Temperature and doping concentration dependence of the energy band gap in  $\beta\text{-Ga}_2\text{O}_3$  thin films grown on sapphire, *Opt. Mat. Express* 7 (2017) 3561
- [61] F. Zhang, Haiou Li, Yi-Tao Cui, Guo-Ling Li, Qixin Guo, evolution of optical properties and band structure from amorphous to crystalline  $\text{Ga}_2\text{O}_3$  films *AIP Advances* 8 (2018) 045112
- [62] Sin-Liang Ou, Dong-Sing Wu, Yu-Chuan Fu, Shu-Ping Liu, Ray-Hua Horng, Lei Liu, Zhe-Chuan Feng, Growth and etching characteristics of gallium oxide thin films by pulsed laser deposition, *Materials Chemistry and Physics* 133 (2012) 700
- [63] F.B. Zhang, Saito, K., Tanaka, T. Nishio, M., Guo, Q. X. structural and optical properties of  $\text{Ga}_2\text{O}_3$  films on sapphire substrates by pulsed laser deposition, *J. of Cryst. Growth* 387 (2014) 96
- [64] K. Matsuzaki, H. Hiramatsu, K. Nomura, H. Yanagi... Growth, structure and carrier transport properties of  $\text{Ga}_2\text{O}_3$  epitaxial film examined for transparent field-effect transistor, *Thin Sol. Films* 496 (2000) 37
- [65] D. Guo, Z. Wu, P. Li, Y. An, H. Liu, X. Guo, H. Yan, G. Wang, C. Sun, L. Li, W. Tang, Fabrication of  $\beta\text{-Ga}_2\text{O}_3$  thin films and solar-blind photodetectors by laser MBE technology *Optical Materials Express* 4 (2014) 106
- [66] D. Y. Guo, Y. P. Qian, Y. L. Su, H. Z. Shi, P. G. Li, J. T. Wu, S. L. Wang, C. Cui, W. H. Tang, Evidence for the bias-driven migration of oxygen vacancies in amorphous non-stoichiometric gallium oxide, *AIP Advances* 7 (2017) 065312
-